

**Supporting Information**

**Tough, Durable and Strongly Bonded Self-Healing Cartilage-mimicking  
Noncovalent Assembly Hydrogel Nanostructures: The Interplay of  
Experiment and Theory**

Shikha Awasthi<sup>1\*</sup>, Sarvesh Kumar Pandey<sup>2\*</sup>, Hulikere Jagdish Shwetha<sup>3</sup>, Nehal<sup>1</sup> and S. Selvaraj<sup>4</sup>

<sup>1</sup>Department of Chemistry, School of Basic Sciences, Manipal University Jaipur, Jaipur – 303007, Rajasthan, India

<sup>2</sup>Department of Chemistry, Maulana Azad National Institute of Technology, Bhopal-462003, Madhya Pradesh, India

<sup>3</sup>Department of Materials Engineering, Indian Institute of Science Bengaluru, Bengaluru - 560012, Karnataka, India

<sup>4</sup>Department of Physics, Saveetha School of Engineering, Saveetha Institute of Medical and Technical Sciences, Thandalam, Chennai-602105, Tamil Nadu, India

Corresponding Authors email:

\*Shikha Awasthi: [awas.shikha2212@gmail.com](mailto:awas.shikha2212@gmail.com)

\*Sarvesh Kumar Pandey: [skpchmiitk@gmail.com](mailto:skpchmiitk@gmail.com)

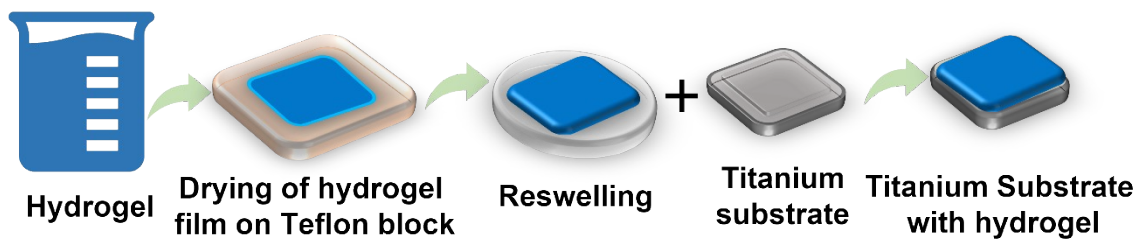


Figure S1: Preparation of hydrogel for electrochemical testing.

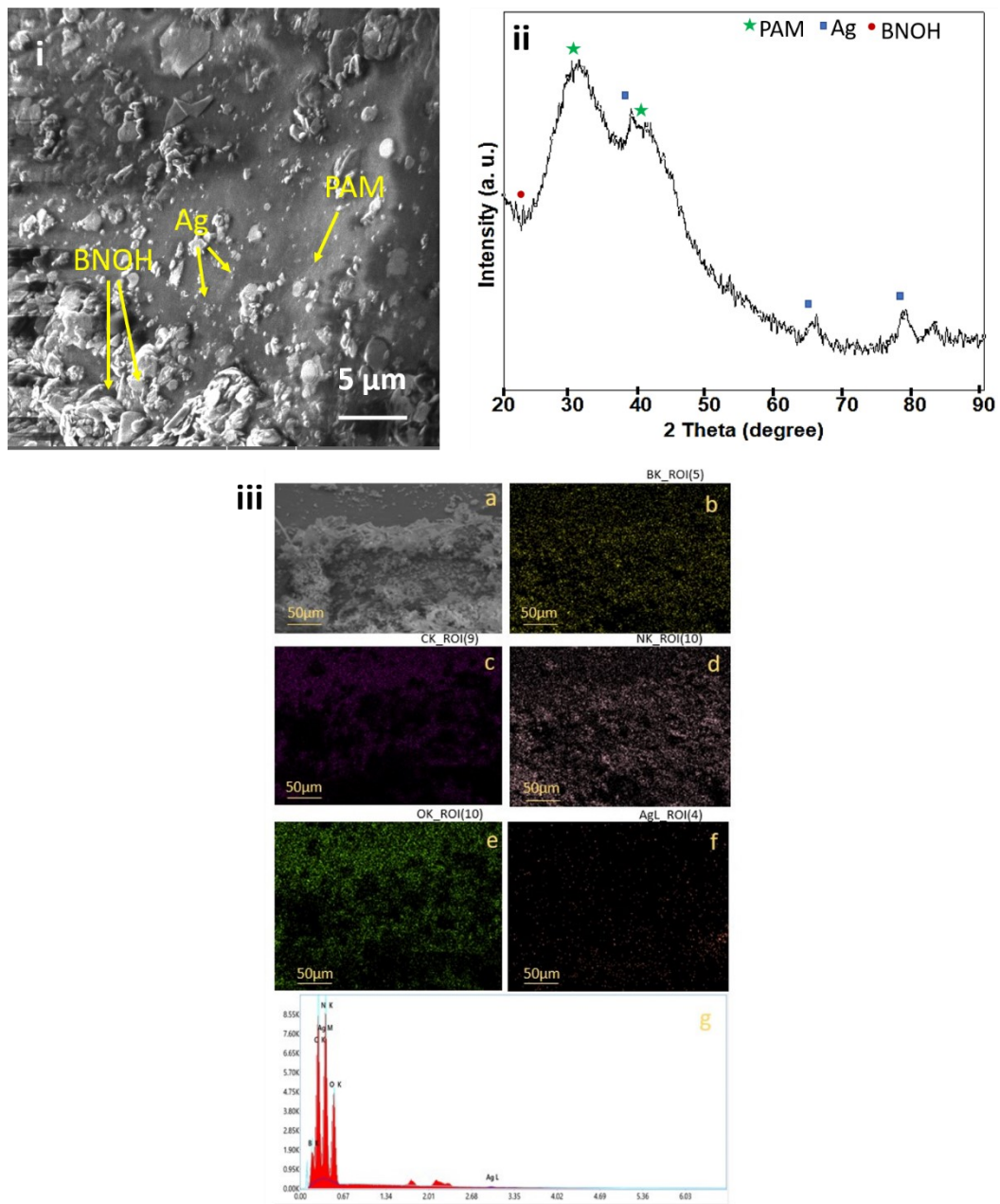


Figure S2A: (i) SEM image, (ii) XRD and (iii) Elemental mapping of PAM-Ag-BN trimer composite showing (a) surface morphology, (b) elemental B distribution, (c) elemental C

distribution, (d) elemental N distribution, (e) elemental O distribution, (f) elemental Ag distribution and (g) EDS.

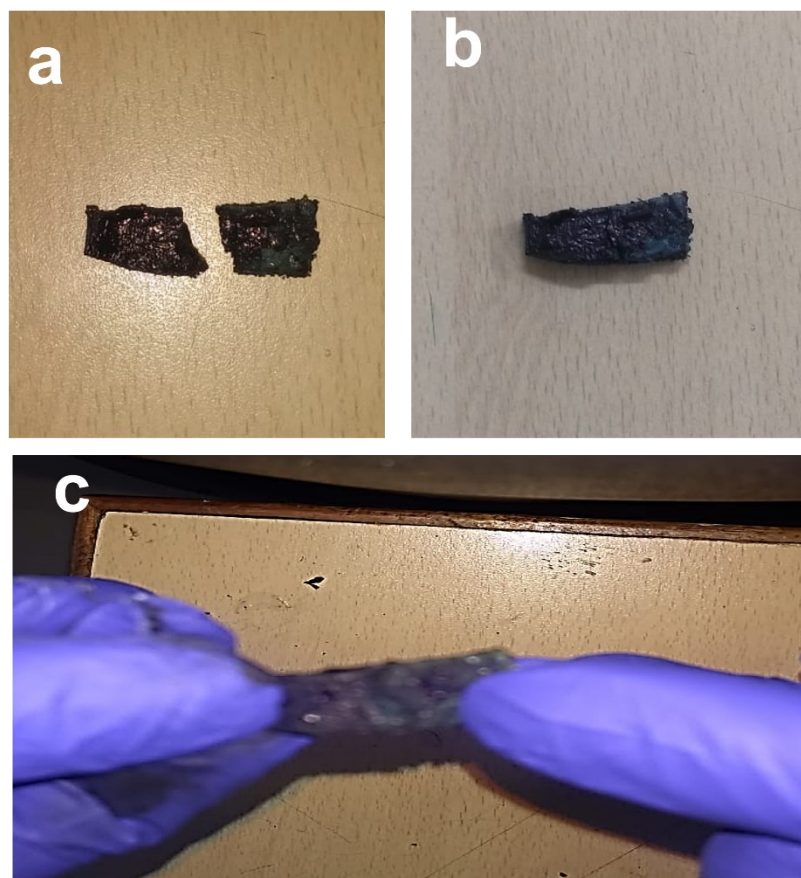


Figure S2B: Images of self-healed sample (a) two halves of PAM-Ag-BN sample, (b) Self-healing of the sample and (c) force applied on the self-healed sample, showing a significant recovery.

### Computational Study - Supporting Information (SI)

**Section S1.** A clear picture of the QTAIM molecular graphs of all the three composite models can be seen in Figures **S3** (Ag), **S4** (PAM), **S5** (BNOH), **S6** (PAM-Ag), **S7** (PAM-BNOH), and **S8** (PAM-Ag-BNOH) which illustrate all binding features [noncovalent (*via* conventional and NBPs) and covalent interactions] involved therein the species. *For the sake of clarity of the graphical visualization of all the MNIs (Ag-O, Ag-N, Ag-H), covalent bond (B-O), NCIs (weak to moderate to strong HBs), and extremely weak vdW interactions, monomer units, dimer and trimer complexes can be seen by viewing these through Zoom (Zoom-In Mode).*

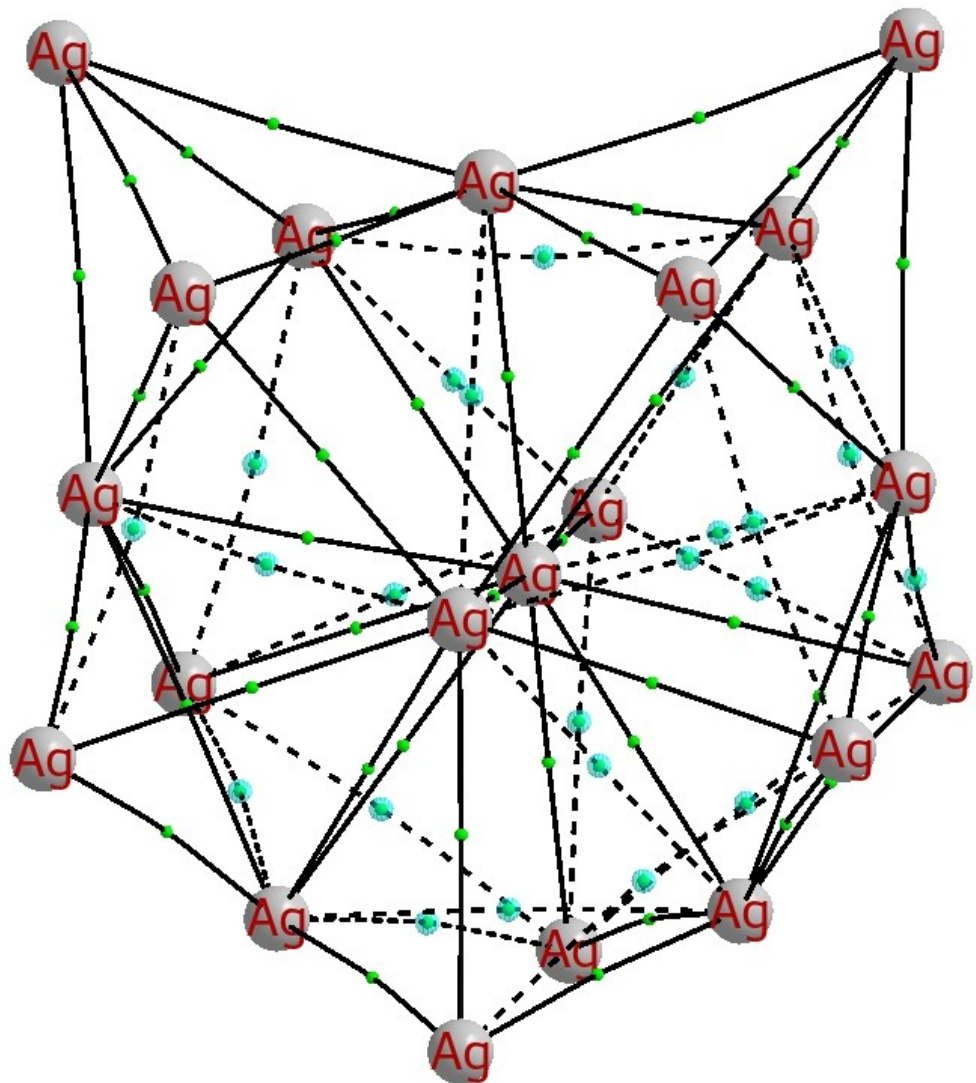
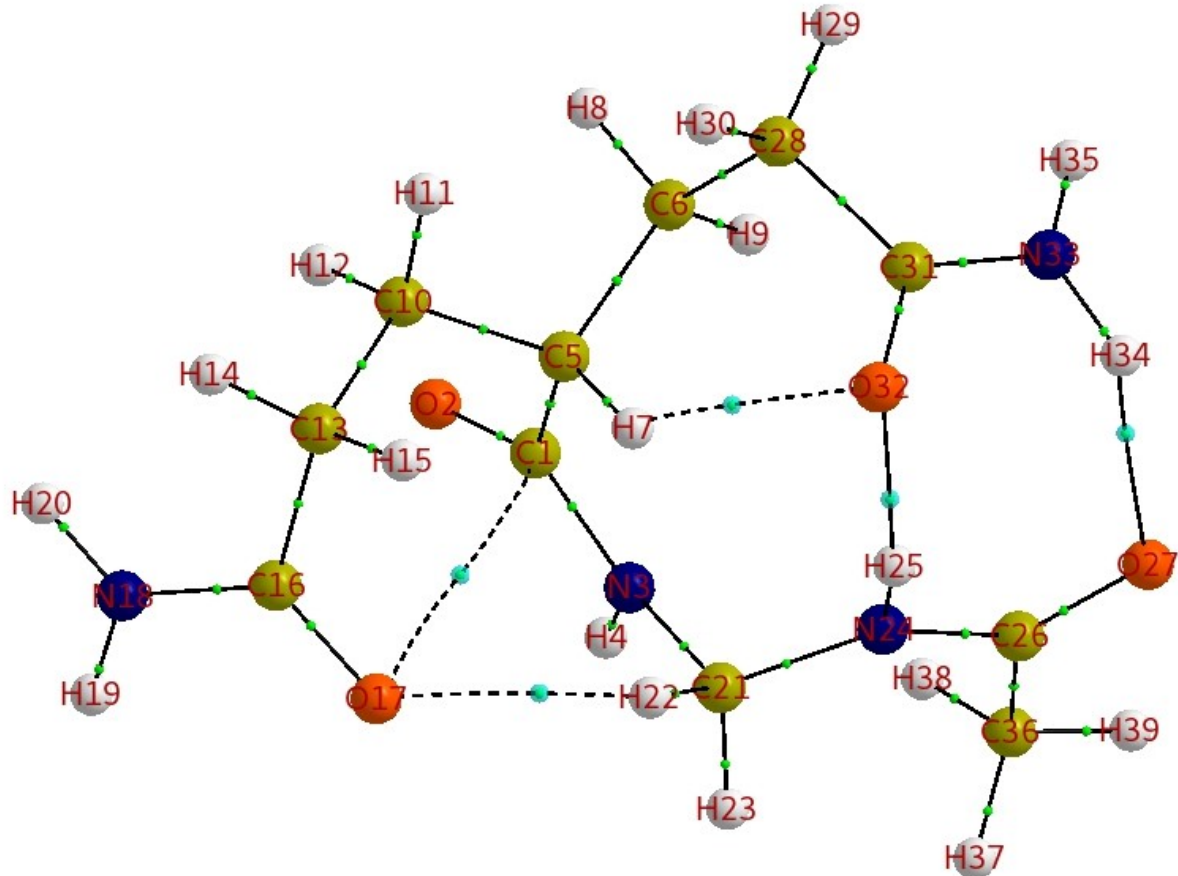


Figure S3: QTAIM-based Molecular Graph of the Ag Assembly as a Component Model.



**Figure S4.** QTAIM-based Molecular Graph for the PAM Monomer Unit Chosen as a Model

**Table S1.** Some Important and Selected QTAIM-based Topological Parameters [ $\rho$ ,  $\nabla^2(\rho)$ ,  $V$ , DI (A, B)] of the PAM Parent (Monomer) Unit

Bond	HBD, BPL (in Å)	$\rho$ (au)	$\nabla^2(\rho)$ (au)	$V$ (au)	DI (A, B)
NCI (Intramolecular)					
N24-H25…O32	1.880, 1.907	0.031	+0.103	-0.027	0.090
N33-H34…O27	1.978, 2.005	0.026	+0.084	-0.022	0.075
C21-H22…O17	2.278, 2.299	0.014	+0.052	-0.011	0.048

C5-H7···O32	2.317, 2.339	0.015	+0.049	-0.011	0.050
NBP (Intramolecular)					
Bond Path	BL, BPL (in Å)	$\rho$ (au)	$\nabla^2(\rho)$ (au)	$V$ (au)	DI (A, B)
C1···O17	3.129, 3.141	0.007	+0.027	-0.005	0.018

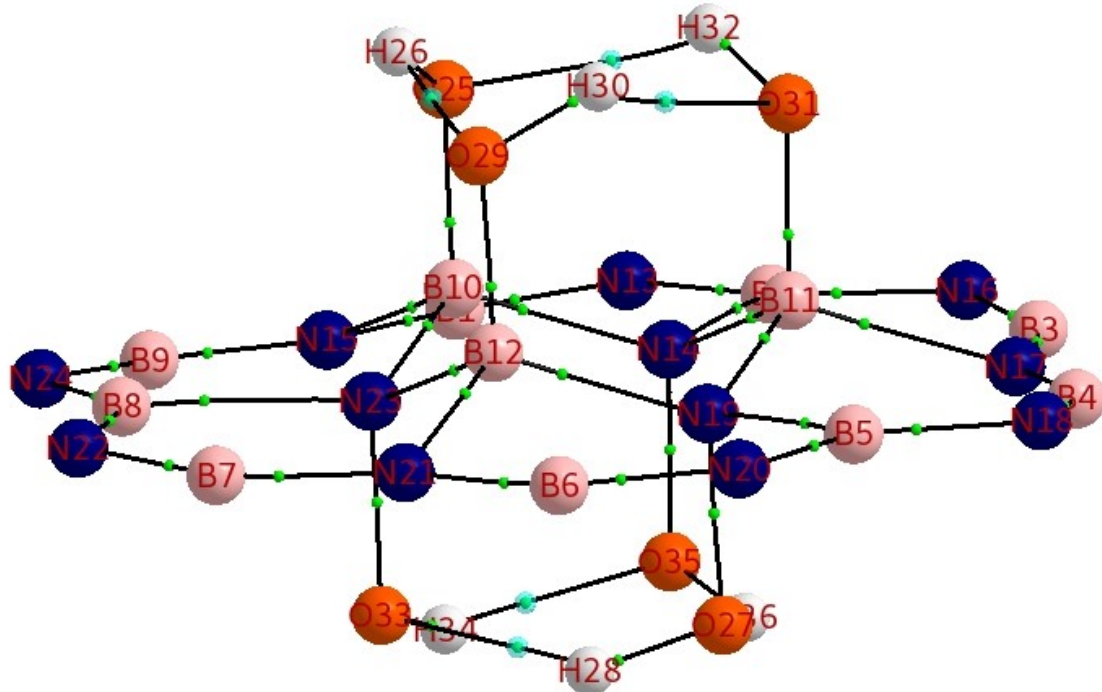


Figure S5. QTAIM-based Molecular Graph for the BNOH Monomer Unit Chosen as a Model

Table S2. Some Important and Selected QTAIM-based Topological Parameters [ $\rho$ ,  $\nabla^2(\rho)$ ,  $V$ , DI (A, B)] of the BNOH Parent (Monomer) Unit

Bond	HBD, BPL (in Å)	$\rho$ (au)	$\nabla^2(\rho)$ (au)	$V$ (au)	DI (A, B)	Region
NCI (Intramolecular)						
O35-H36···O27	1.806, 1.825	0.041	+0.131	-0.037	0.096	N-side (bottom)
O27-H28···O33	1.810, 1.829	0.040	+0.130	-0.037	0.095	N-side (bottom)

O33-H34···O35	1.811, 1.830	0.040	+0.129	-0.037	0.095	N-side (bottom)
O25-H26···O29	1.992, 2.019	0.028	+0.091	-0.025	0.065	B-side (top)
O31-H32···O25	1.996, 2.023	0.027	+0.090	-0.025	0.065	B-side (top)
O29-H30···O31	2.001, 2.029	0.027	+0.089	-0.025	0.064	B-side (top)

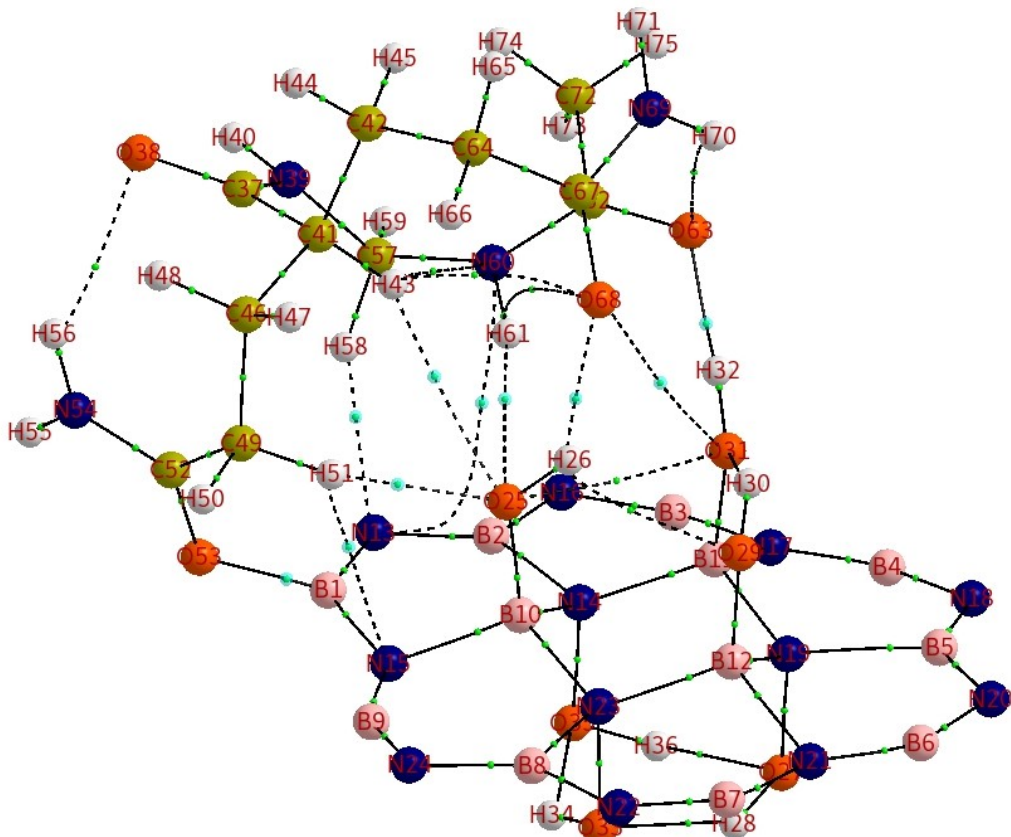


Figure S6. QTAIM-based Molecular Graph for the PAM-BNOH Composite Model

**Table S3.** Some Important and Selected QTAIM-based Topological Parameters [ $\rho$ ,  $\nabla^2(\rho)$ ,  $V$ , DI (A, B)] of the PAM-BNOH Composite Model

Bond	BL, BPL (in Å)	$\rho$ (au)	$\nabla^2(\rho)$ (au)	$V$ (au)	DI (A, B)
Covalent bond Between the PAM and BNOH Components					
B1-053	1.564, 1.568	0.107	+0.404	-0.213	0.314

NCI (Intermolecular) Between the PAM and BNOH Components					
Bond	HBD, BPL (in Å), bond angle	ρ (au)	∇² (ρ) (au)	V (au)	DI (A, B)
O31-H32…O63	1.710, 1.738, 174.1°	0.045	+0.148	-0.039	0.115
O25-H26…O68	1.924, 1.950, 136.1°	0.024	+0.101	-0.023	0.051
C49-H51…O25	2.087, 2.105, 176.7°	0.022	+0.070	-0.019	0.072
C41-H43…O25	2.792, 2.815, 143.8°	0.005	+0.020	-0.003	0.015
C57-H58…N13	2.135, 2.155, 151.1	0.023	+0.066	-0.016	0.100
C49-H51…N15	2.603, 2.634, 124.7°	0.010	+0.039	-0.007	0.023
N60-H61…O25	2.520, 2.546, 169.3°	0.008	+0.030	-0.006	0.026
NBP (Intermolecular) Between the PAM and BNOH Components					
Bond Path	BL, BPL (in Å)	ρ (au)	∇² (ρ) (au)	V (au)	DI (A, B)
O68 – O31	3.187, 3.202	0.005	+0.023	-0.004	0.021
N60 – N13	3.401, 4.002	0.007	+0.023	-0.004	0.017

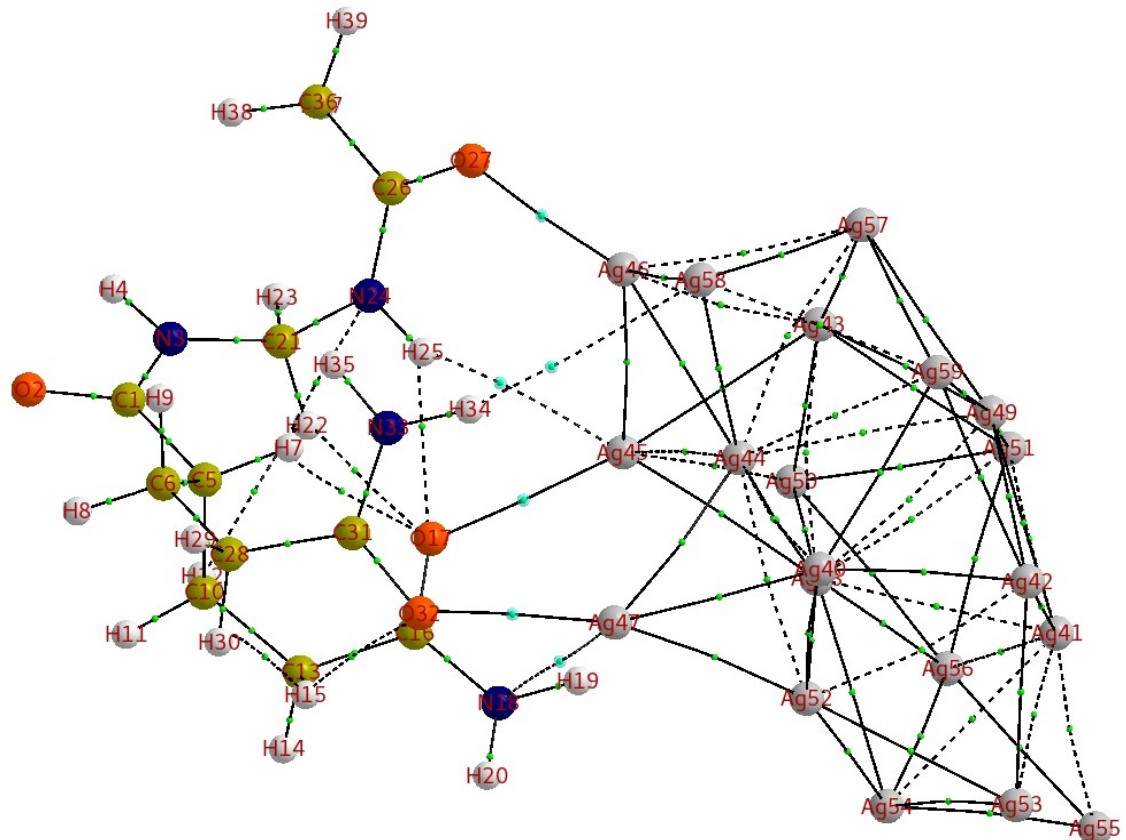


Figure S7. QTAIM-based Molecular Graph for the PAM-Ag Composite Model

**Table S4.** Some Important and Selected QTAIM-based Topological Parameters [ $\rho$ ,  $\nabla^2(\rho)$ ,  $V$ , DI (A, B)] of the PAM-Ag Composite Model

Bond	BL, BPL (in Å)	$\rho$ (au)	$\nabla^2(\rho)$ (au)	$V$ (au)	DI (A, B)
MNI (Intermolecular) Between the PAM and Ag Assembly Components					
Ag47-O32	2.362, 2.365	0.043	+0.227	-0.055	0.301
Ag46-O27	2.411, 2.415	0.039	+0.197	-0.047	0.283
Ag45-O17	2.554, 2.557	0.030	+0.133	-0.032	0.224
Ag45···H25	2.751, 2.780	0.008	+0.026	-0.005	0.025
Ag58···H34	3.222, 3.303	0.005	+0.011	-0.002	0.027
Ag47···N18	3.706, 3.713	0.004	+0.011	-0.002	0.028

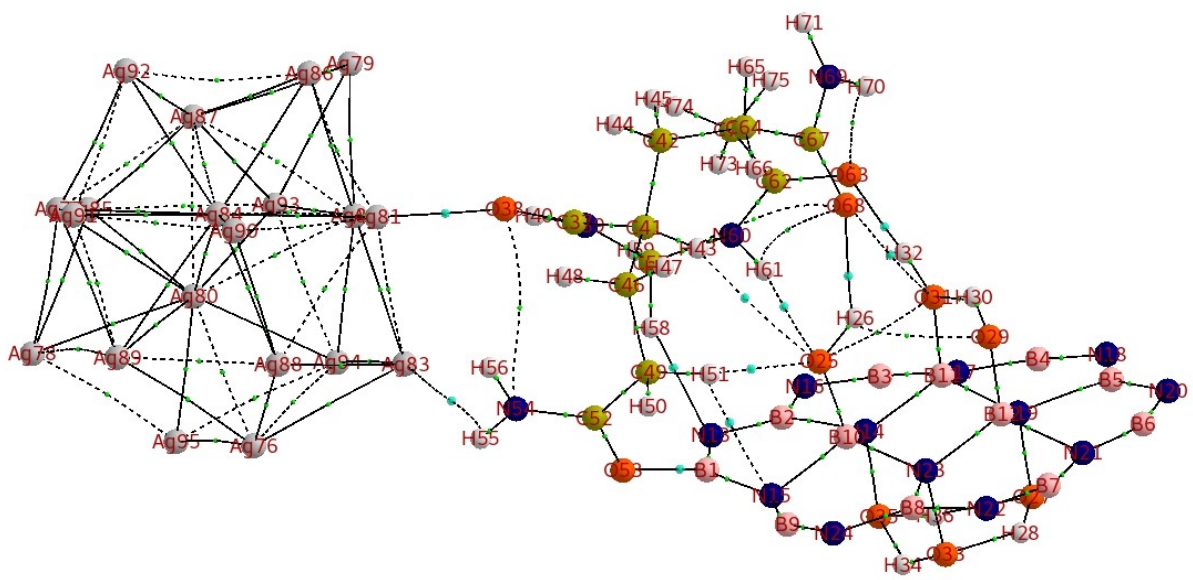


Figure S8. QTAIM-based Molecular Graph for the PAM-Ag-BNOH Composite Model

Table S5. Some Important and Selected QTAIM-based Topological Parameters [ $\rho$ ,  $\nabla^2(\rho)$ ,  $V$ , DI (A, B)] of the PAM-Ag-BNOH Composite Model

Bond	BL, BPL (in Å)	$\rho$ (au)	$\nabla^2(\rho)$ (au)	$V$ (au)	DI (A, B)
MNI (Intermolecular) Between the PAM and Ag Units					
Ag81-O38	2.398, 2.401	0.040	+0.205	-0.049	0.290
Ag83···H55	3.168, 3.240	0.005	+0.012	-0.002	0.020
Covalent Bond (Intermolecular) Between the PAM and BNOH Components					
B1-O53	1.558, 1.562	0.109	+0.422	-0.217	0.315
NCI (Intermolecular) Between the PAM and BNOH Components					
Bond	HBD, BPL (in Å), bond angle	$\rho$ (au)	$\nabla^2(\rho)$ (au)	$V$ (au)	DI (A, B)
O31-H32···O63	1.722, 1.750, 174.3°	0.043	+0.143	-0.038	0.113
O25-H26···O68	1.912, 1.978, 136.4°	0.025	+0.104	-0.024	0.052

C49-H51…O25	2.079, 2.097, 170°	0.023	+0.071	-0.019	0.073
C41-H43…O25	2.787, 2.810, 144.4°	0.005	+0.021	-0.003	0.015
C57-H58…N13	2.079, 2.099, 151.3°	0.026	+0.075	-0.018	0.107
C49-H51…N15	2.594, 2.625, 124.1°	0.010	+0.040	-0.007	0.023
N60-H61…O25	2.500, 2.526, 168.9	0.008	+0.031	-0.006	0.027
NBP (Intermolecular) Between the PAM and BNOH Units					
Bond Path	BL, BPL (in Å)	ρ (au)	∇² (ρ) (au)	V (au)	DI (A, B)
O31 - O68	3.142, 3.154	0.006	+0.025	-0.005	0.024

## Section S2. NCI-Plot: 2D Scatter Plot and 3D Isosurface Map

A full description about the NCI-plot can be seen in the literature in understanding and plotting of the NCIs in a better way [Contreras-García, J.; Johnson, E. R.; Keinan, S.; Chaudret, R.; Piquemal, J. P.; Beratan, D.N.; Yang, W. NCIPILOT: A Program for Plotting Noncovalent Interaction Regions. *J. Chem. Theory Comput.* **2011**, *7* (3), 625–632; Johnson, E. R.; Keinan, S.; Mori-Sánchez, P.; Contreras-García, J.; Cohen, A. J.; Yang, W. Revealing Noncovalent Interactions. *J. Am. Chem. Soc.* **2010**, *132* (18), 6498–6506]. As reported by Yang *et al* [Johnson, E. R.; Keinan, S.; Mori-Sánchez, P.; Contreras-García, J.; Cohen, A. J.; Yang, W. Revealing Noncovalent Interactions. *J. Am. Chem. Soc.* **2010**, *132* (18), 6498–6506], deep insights into the electron density and its derivatives-based method can be viewed the published work as cited above. A detailed evaluation of the NCI-plot on a few bio-composite materials can be seen in literature [Bio-composites taken as the PAM-TiO<sub>2</sub>, PAM-CNT, PAM-TiO<sub>2</sub>-CNT - S. Awasthi, J. Gaur, S. K. Pandey, M. S. Bobji, and C. Srivastava, High Strength, Strongly Bonded Nanocomposite Hydrogels for Cartilage Repair *ACS App. Mat. Int.* **13**, (2021), 24505-24523; Bio-composites takes as the HAP-BN, HAP-CNT, and HAP-GrO - S. Awasthi, J. Gaur, S. K. Pandey, and C. Srivastava, Load-bearing study and interfacial interactions of hydroxyapatite composite coatings for bone tissue engineering, *Mater. Chem. Front.* **6**, (2022), 3731-3747] and references therein.

**Hints:** The RDG isosurface displayed on horizontal axis is 0.5 (ranging from -0.05 to +0.05). The  $\Omega(r)$  values ranging from -0.035 atomic unit (au) to +0.02 au on vertical axis (Figure 10, right) show the color surfaces of the species on a blue-green-red scale. The detailed description of the NCI tool clarifies that the higher density values ( $\Omega(r) < 0$ ) show the stronger attractive interactions while the very low-density values ( $\Omega(r) > 0$ ) indicate the repulsive interactions. Moreover, blue color spike in the scatter map two-dimensional (2D) plot and blue color disc-shaped NCI isosurface three-dimensional

(3D) representation showing the attractive (stabilizing) interaction. The green color spikes in the 2D scatter plot and green color disc-shaped NCI 3D isosurface demonstrating a variety of vdW interactions. The presence of steric effect is evidently shown by the low-gradient spikes appearing at positive side. This effect as shown by the red ellipsoid depicts the electron density depletion which is because of the electrostatic repulsion.